Optics Letters

Highly efficient 3.7 kW peak-power single-frequency combined Er/Er-Yb fiber amplifier

M. M. Khudyakov,[1,2,*] D. S. Lipatov,[3] A. N. Gur'yanov,[3] M. M. Bubnov,[1] and M. E. Likhachev[1]

[1]Fiber Optics Research Center of the Russian Academy of Sciences, 38 Vavilov Street, Moscow 119333, Russia
[2]Moscow Institute of Physics and Technology, 9 Institutskiy per., Dolgoprudny, Moscow Region 141700, Russia
[3]Institute of Chemistry of High Purity Substances of the Russian Academy of Sciences, 49 Tropinin Street, Nizhny Novgorod 603950, Russia
*Corresponding author: DAngeL.74@gmail.com

Received 24 December 2019; revised 14 February 2020; accepted 18 February 2020; posted 18 February 2020 (Doc. ID 386831); published 19 March 2020

In this Letter, we propose and realize a novel concept for a high-peak-power highly efficient fiber amplifier in the 1.55 μm spectral range. The amplifier is based on the simultaneous utilization of Er-doped, Yb-free, and Er-Yb codoped large-mode-area fibers spliced together. Using this approach, we demonstrate the amplification of single-frequency 160 ns pulses at 1554 nm to a peak power of 3.7 kW with a pump-to-signal conversion efficiency of 23.6% relative to the launched multimode pump power at 976 nm.

https://doi.org/10.1364/OL.386831

Single-frequency high-peak-power pulsed lasers operating in the eye-safe 1.55 μm spectral range are required in many free-space applications, such as Doppler wind LIDAR and gas column sensing [1,2]. A good beam quality ($M2 < 1.5$) and a high pulse energy are needed for such applications to achieve a high signal-to-noise ratio for a large scanning distance. At the same time, single-frequency pulses must be reasonably short (100 s of nanoseconds) to provide a good spatial resolution. The main factor limiting the peak power of such pulses is stimulated Brillouin scattering (SBS) [3]. The best candidates for these applications are fiber lasers due to their diffraction-limited beam quality (in the case of single-mode fibers) and superior stability (in the case of an all-fiber design). However, the large interaction length in the optical fibers decreases the thresholds of the SBS. The utilization of large-mode-area (LMA) active fibers allows one to increase the SBS threshold. However, to achieve a reasonably high peak power for single-frequency pulses, it is also necessary to use very short active fibers, which have a negative impact on the pump-to-signal conversion efficiency (PCE).

The three main amplifier types operated near 1.55 μm are the cladding-pumped Er-Yb fiber (EYDF) amplifier, the cladding-pumped Er-doped (Yb-free) fiber (EDF) amplifier, and the core-pumped EDF. To illustrate the difficulty of obtaining a high peak power with a high efficiency, in Fig. 1, we plot the PCE against the output peak power of single-frequency pulses for the different amplifiers designs [4–18]. To date, the highest peak power of 4 kW for single-frequency single-mode pulses was demonstrated in a cladding-pumped EDF with a copropagating pump and signal [4]. This peak power was achieved at the expense of a PCE reduction from 40% for the continuous-wave (CW) regime [5] down to 5%. The EDF length was only 1 m in the last case. The same setup with a longer fiber length (~3 m) reduced the peak power to 1 kW and increased the PCE to 12%. A counterpropagating pumping scheme allowed for a further increase in the PCE up to 16.5% without a reduction in the peak power [6]. The highest PCE of 46% for the cladding-pumped amplifiers was demonstrated using an EYDF in a counterpropagating scheme with off-resonant pumping at 940 nm [16]. However, the utilization of an EYDF for pulsed amplifiers results in a PCE of 16.7% for a 1 kW peak power [9] and 3% for 3.5 kW [10], which is even lower than the PCE for the EDF at similar peak powers. A core-pumped EDF at 1480 nm demonstrated a PCE of 30% for 0.7 kW [7] and 71% for the CW regime [8]. However, the Raman laser at 1480 nm used as a pump source in Refs. [7,8] can have a maximum PCE of no more than 42% [19] relative to semiconductor multimode pump diodes. Thus, in the case of the core-pumped EDF amplifiers, the full optical-to-optical PCE (relative to the power of multimode pump diodes) is lower than that of the cladding-pumped EDF and EYDF schemes.

The main factor limiting the PCE of the EDF amplifiers operating at a high peak power is the low pump absorption [see the signal and pump power distributions over the EDF for the copropagating pump and signal scheme in Fig. 2(a)]. In this case, the maximum Er^{3+} ion concentration is limited by concentration quenching [20], so the highest pump-to-signal conversion efficiency for a short EDF is achieved when a significant part of the pump is unabsorbed [4].

Yb codoping can solve this problem, since the Yb^{3+} ions have almost an order of magnitude higher absorption cross section near 1 μm and can efficiently transfer the excitation to the

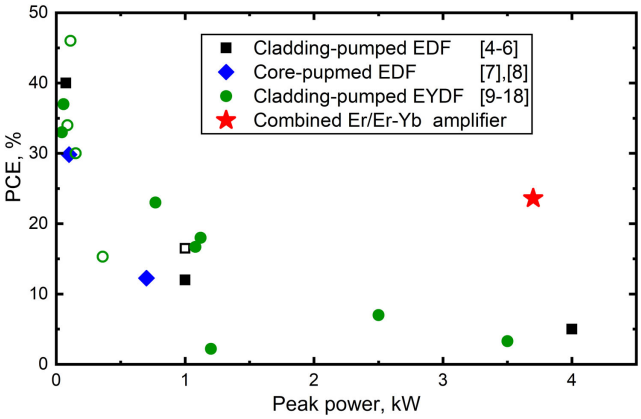

Fig. 1. PCE (relative to the multimode pump diode power) versus the maximum achieved peak power for various amplifier schemes: the solid symbols correspond to copropagating schemes, and the open symbols correspond to counterpropagating schemes.

nearby Er^{3+} ions. Nonetheless, the LMA EYDFs in the copropagating scheme require a very high input power to achieve a saturation with the input signal [see Figs. 2(b) and 2(c)]. The reason for that is a high population inversion of Er^{3+} ions for a small signal and a high pump power. In this case the probability of upconversion due to the transfer of energy from Yb^{3+} ion to exited Er^{3+} ion become very high, which results in a loss of a pump photon and a reduction of the overall PCE. The output power of a preamplifier is limited by a much lower SBS threshold, which leads to either a low PCE [9,10,14] or cumbersome cladding-pumped preamplifiers [9,10]. Counterpropagating pumping schemes require a smaller seed power to saturate the EYDF, but the additional passive fiber length (in a pump and signal combiner) at the output of the amplifier limits the maximum peak power of an all-fiber design (see Fig. 1).

In this Letter, we propose to mitigate the low pump absorption of the EDF and the high input power requirement of the EYDF by splicing an EYDF directly after an EDF, thus creating a combined fiber amplifier. In this scheme, the EDF acts as a preamplifier for the EYDF by boosting the low input signal (<100 mW) to a level of several watts with a high PCE relative to the absorbed pump power. The unabsorbed pump power from the EDF is nearly completely absorbed in the EYDF, which operates in a saturation regime with a high PCE. Therefore, the whole PCE of the combined amplifier is also high. An additional benefit of this approach is the ability to increase the SBS threshold by choosing an EDF and an EYDF with the different SBS shifts (different core compositions).

The EDF used in this Letter is similar to the one reported in Ref. [4]. The preform of this fiber was manufactured by a modified chemical vapor deposition technique. The core of the fiber was based on a P_2O_5–Al_2O_3–SiO_2 glass matrix and codoped with 0.1 mol.% Er_2O_3. The preform was polished to a square shape and drawn into a fiber with the outer dimensions of 110 μm × 110 μm. The core diameter is approximately 35 μm, and the calculated cut-off wavelength and mode field diameter at $1/e^2$ are 1650 nm and 24.7 μm, respectively. This resulted in a robust single-mode performance for a bend diameter of 30 cm. The fiber was coated with a low-index polymer, which provided a numerical aperture (NA) of 0.46. The measured small-signal

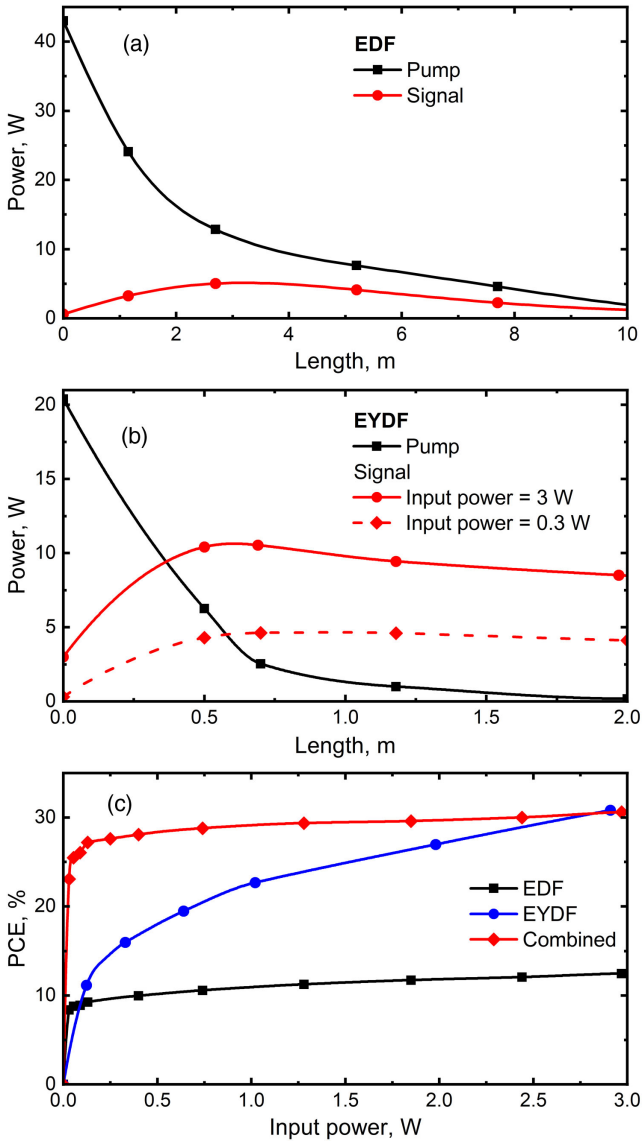

Fig. 2. Measured signal (1557 nm) and pump (976 nm) distributions along the cladding-pumped (a) EDF (similar to the one reported in Ref. [4]) and (b) EYDF (Nufern LMA-EYDF-25 P/300-HE) lengths at different input powers and (c) PCE versus input power @ 1557 nm for a 1.5 m cladding-pumped EDF, 0.5 m EYDF and the combined amplifier consisting of 1.5 m EDF and 0.5 m EYDF.

absorption from the cladding at a pump wavelength of 976 nm was 2 dB/m (peak absorption at 981 nm was 2.7 dB/m).

We used commercially available LMA-EYDF-25 P/300-HE, Nufern fiber for the EYDF. The fiber core was doped with 12 mol.% P_2O_5, 7 wt.% Yb_2O_3 and 0.45 wt.% Er_2O_3 [21]. The fiber had a pedestal doped with 10 mol.% GeO_2 around the core to reduce core-clad NA down to ~ 0.09. As a result, this fiber had a mode field diameter of 18 μm and a calculated core cut-off wavelength of 3050 nm relative to the pedestal. It had an octagonal outer cladding shape and was coated with a low-index polymer with an NA of 0.46. A nearly single-mode operation regime was achieved by coiling the EYDF around an aluminum cylinder with an outer diameter of 8 cm. The measured peak small-signal absorption at 976 nm was 14.3 dB/m. Such a high

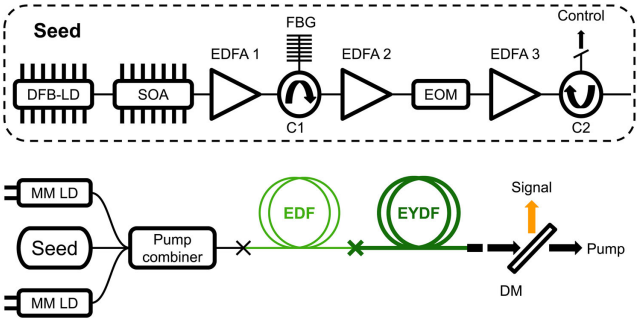

Fig. 3. Schematic of the combined amplifier setup.

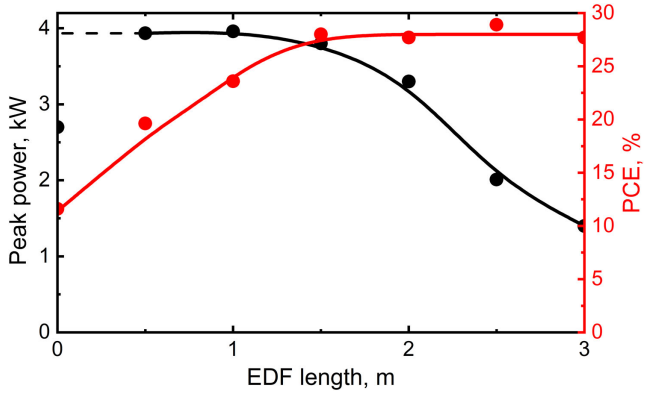

Fig. 4. Measured SBS threshold and the PCE versus EDF length.

absorption leads to a high heat load on the fiber. In our experiment, we employed active air cooling of the input end of the fiber, as well as the passive cooling provided by the aluminum cylinder. Nevertheless, to prevent thermal damage to the EYDF, we limited the pump power reaching the fiber to 25 W.

A schematic of the combined amplifier in this work is presented in Fig. 3. A semiconductor optical amplifier (SOA) was used to create pulses from the signal of a distributed feedback laser diode (DFB-LD) with a wavelength of 1554 nm, a linewidth of 2 MHz, and an average power of 1 mW with pulse durations varying from 70 ns to 160 ns, repetition rates from 1 kHz up to 100 kHz, and a peak power of 10 mW. This resulted in pulses with an average power of several microwatts. The pulses were amplified by two core-pumped EDF amplifiers (EDFA1, EDFA2) at 976 nm with a spectral filter in between consisting of a circulator (C1) and a fiber Bragg grating (FBG) to remove large amounts of amplified spontaneous emission (ASE) after EDFA1 due to the very low input signal. An electro-optic modulator (EOM) was used to further reduce the amount of power between the pulses and preshape them to achieve a square output pulse shape from the whole setup. This resulted in an average power of 0.5–2 mW and a peak power of up to 2 W.

The signal was further amplified by an LMA cladding-pumped EDF amplifier (EDFA3) to achieve an average power of 80–200 mW and a peak power of up to 100 W. We used a high-power circulator (C2) to control the backscattered light from the combined amplifier. The signal was launched into the EDF with up to 60 W of pump power from wavelength-stabilized multimode laser diodes (MM LDs) at 976 nm through a $2+1:1$ pump-to-signal combiner. The EDF was directly spliced with the EYDF. To prevent a Fresnel reflection from the output fiber end, we added an end cap due to the very high NA of the pedestal in the EYDF. We used a dichroic mirror (DM) to separate the amplified signal from the residual pump. An integrating photodetector (IPD) [22] was used to control part of the ASE and accurately derive the resulting peak power.

The measurements of the SBS shift in the fibers with core compositions similar to those of the EDF and EYDF but without Er (to avoid a high signal loss in the long fiber used in our setup) have shown that the SBS spectra of the chosen fibers do not intersect with each other (the SBS shift for the EDF was estimated to be ~10.7 GHz, and the SBS shift for the EYDF was estimated to be ~10.2 GHz). Thus, the SBS threshold of the combined amplifier is defined by the smallest SBS threshold of one of the fibers (EDF or EYDF).

We chose an optimal EYDF length of 0.5 m for a high input signal [see Fig. 2(b)]. To choose the optimal length of the EDF, we conducted a set of experiments on the combined amplifier varying the EDF length (see Fig. 4). We measured the SBS threshold power for 70 ns pulses by observing the onset of the pulse instability (oscillations near the trailing edge of the pulse) and measuring the backscattered light from the amplifier. The PCE was measured at a high repetition rate to operate well below the SBS threshold and maximal energy of the amplifier. It is worth noting that our seed source was unable to provide enough power to achieve the SBS threshold without an Er fiber due to the low PCE of the EYDF (11.6%) and 25 W pump limit. However, we can conclude that leveling off the SBS threshold with a decrease in the EDF length means that SBS in the EYDF limits the peak power when the EDF is shorter than 1 m. Therefore, the SBS threshold in a 0.5 m long EYDF can be estimated to be approximately 4 kW. It is worth noting that such a high threshold is consistent with [13,18] with respect to used fiber length. An increase in the EDF length beyond 1.5 m does not lead to an increase in the PCE beyond the accuracy of the PCE measurement. Thus, the optimal length of the EDF was determined to be 1.5 m.

With an EDF length of 1.5 m, the limit of the pump power was 45 W. The repetition rate was 20 kHz. Part of the ASE in the output signal was measured both by the IPD and a spectrum analyzer and was found to be below 1% for pump powers below 40 W and 3% at 45 W [see Fig. 5(c)]. The ASE in the spectral range around 1 μm was less than 1 mW, corresponding to the very low Yb ASE observed in Ref. [11]. A total output power of 9.6 W (9.3 W after the ASE correction) was achieved. The PCE was determined to be 23.6%. At the maximal pump power, the pulse energy was about 460 μJ [see Fig. 5(a)], and the FWHM was 157 ns. The SBS threshold was determined by observing the trailing edge oscillations, which can be seen as a small dip at the trailing edge of the pulse in Fig. 5(b). An M^2 value of 1.34/1.35 was measured with a Thorlabs M2MS-BP209IR/M setup. The beam profile image [see the inset in Fig. 5(b)] also indicates a good beam quality.

It is worth noting that the combined Er/Er-Yb amplifier has high efficiency for a very high signal gain. To demonstrate the advantage of the proposed design, we measured the saturation curves [see the dependence of the PCE on the input signal for a fixed maximum pump power in Fig. 2(c)]. As mentioned above, a single Er-Yb amplifier (fiber length of 0.5 m) can demonstrate a rather high PCE but requires a very high input signal of a few W and a rather low gain of a few dB. The behavior of the cladding-pumped EDF (length of 1.5 m) is opposite:

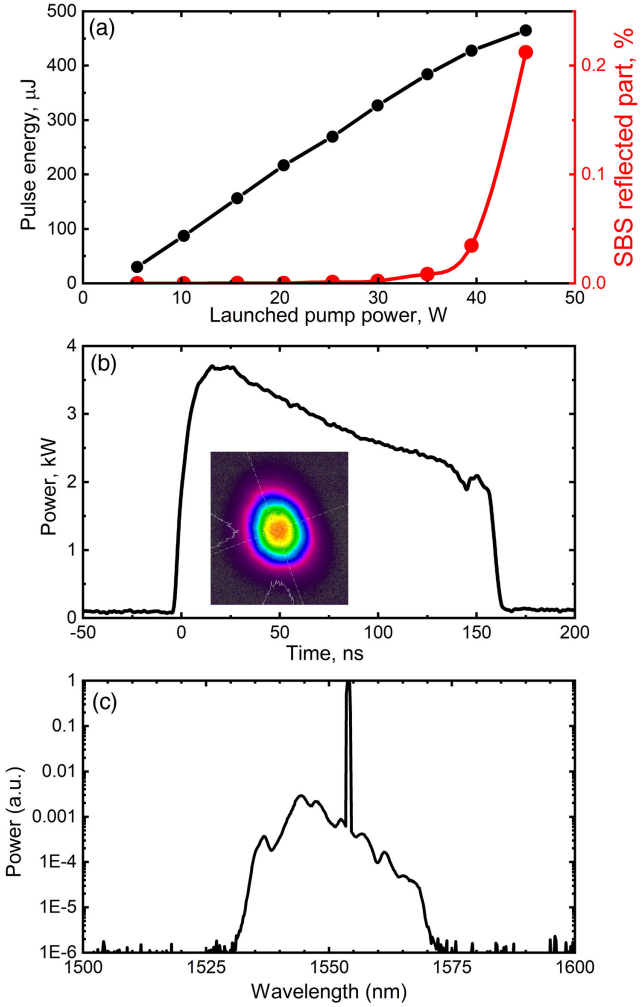

Fig. 5. (a) Pulse energy and reflected by SBS percent of the output power. (b) Output pulse shape at maximal pump power; the inset shows a near-field beam profile image measured with a Spiricon SP-1550M camera. (c) Spectrum at the amplifier output at maximal pump power.

a very small input signal is required to saturate the amplifier, but the maximum PCE is small compared to that of the Er-Yb amplifier. The combined Er/Er-Yb amplifier demonstrates the benefits of both schemes: it has a low saturation input power of only ~100 mW but simultaneously has a very high PCE. This behavior makes the concept of a combined amplifier even more appealing.

It is worth noting that if a record high peak power is not required, an even higher PCE can be achieved in the combined Er/Er-Yb amplifier. Indeed, by simple increases in the EYDF length to 1.2 m and EDF length to 1.8 m, we obtained a peak power of 1 kW with a PCE of 30.9%. Moreover, for a peak power of 1 kW EDF length can be increased to 3 m, and the Er concentration can be reduced, which should result in an increase in the PCE relative to the absorbed pump power. Thus, we expect that after an optimization of the EDF parameters, a peak power of approximately 1 kW and a PCE close to 40% might be achieved. The beam quality M^2 might also be close to unity if a real single-mode EYDF is used [23].

In conclusion, we have proposed and implemented the concept of a monolithic combined Er/Er-Yb fiber amplifier. We demonstrated the amplification of 160 ns pulses to a peak power of 3.7 kW with a PCE of 23.6%. To the best of our knowledge, the demonstrated PCE is more than 4 times higher than the PCE previously achieved in a single EDF amplifier [4] and 7 times higher than the PCE achieved in a single EYDF amplifier [10] for similar peak power levels with single-frequency pulses.

Funding. Russian Science Foundation (18-19-00687).

Disclosures. The authors declare no conflicts of interest.

REFERENCES

1. Y. L. Pichugina, R. M. Banta, W. A. Brewer, S. P. Sandberg, and R. M. Hardesty, J. Appl. Meteorol. Climatol. **51**, 327 (2012).
2. J. B. Abshire, H. Riris, G. R. Allan, C. J. Weaver, J. Mao, X. Sun, W. E. Hasselbrack, A. Yu, A. Amediek, Y. Choi, and E. V. Browell, Proc. SPIE **7832**, 78320D (2010).
3. E. P. Ippen and R. H. Stolen, Appl. Phys. Lett. **21**, 539 (1972).
4. L. V. Kotov, M. E. Likhachev, M. M. Bubnov, V. M. Paramonov, M. I. Belovolov, D. S. Lipatov, and A. N. Guryanov, Laser Phys. Lett. **11**, 095102 (2014).
5. L. V. Kotov, M. E. Likhachev, M. M. Bubnov, O. I. Medvedkov, M. V. Yashkov, A. N. Guryanov, J. Lhermite, S. Février, and E. Cormier, Opt. Lett. **38**, 2230 (2013).
6. L. Kotov, M. Likhachev, M. Bubnov, D. Lipatov, and A. Guryanov, Eur. Conf. Lasers Electro-Optics **095102**, 141700 (2014).
7. J. W. Nicholson, A. DeSantolo, M. F. Yan, P. Wisk, B. Mangan, G. Puc, A. W. Yu, and M. A. Stephen, Opt. Express **24**, 19961 (2016).
8. V. R. Supradeepa, J. W. Nicholson, and K. Feder, in *2012 Conference on Lasers and Electro-Optics (CLEO)* (IEEE, 2012), Vol. **1**, pp. 1–2.
9. X. Zhang, W. Diao, Y. Liu, J. Liu, X. Hou, and W. Chen, Appl. Phys. B **115**, 123 (2014).
10. W. Lee, J. Geng, S. Jiang, and A. W. Yu, Opt. Lett. **43**, 2264 (2018).
11. X. Bai, Q. Sheng, H. Zhang, S. Fu, W. Shi, and J. Yao, IEEE Photonics J. **7**, 1 (2015).
12. P. Kaczmarek, D. Stachowiak, and K. Abramski, Appl. Sci. **8**, 869 (2018).
13. W. Renard, T. Robin, B. Cadier, J. Le Gouët, L. Lombard, A. Durecu, P. Bourdon, and G. Canat, in *CLEO: 2015* (Optical Society of America, 2015), p. STh4L.6.
14. W. Shi, E. B. Petersen, Z. Yao, D. T. Nguyen, J. Zong, M. A. Stephen, A. Chavez-Pirson, and N. Peyghambarian, Opt. Lett. **35**, 2418 (2010).
15. C. Alegria, Y. Jeong, C. Codemard, J. K. Sahu, J. A. Alvarez-Chavez, L. Fu, M. Ibsen, and J. Nilsson, IEEE Photon. Technol. Lett. **16**, 1825 (2004).
16. O. De Varona, W. Fittkau, P. Booker, T. Theeg, M. Steinke, D. Kracht, J. Neumann, and P. Wessels, Opt. Express **25**, 24880 (2017).
17. Y. Jeong, J. K. Sahu, D. B. S. Soh, C. A. Codemard, and J. Nilsson, Opt. Lett. **30**, 2997 (2005).
18. C. E. Dilley, M. A. Stephen, and M. P. Savage-Leuchs, Opt. Express **15**, 14389 (2007).
19. V. R. Supradeepa and J. W. Nicholson, Opt. Lett. **38**, 2538 (2013).
20. M. E. Likhachev, M. M. Bubnov, K. V. Zotov, D. S. Lipatov, M. V. Yashkov, and A. N. Guryanov, Opt. Lett. **34**, 3355 (2009).
21. M. M. Khudyakov, D. S. Lipatov, A. N. Guryanov, M. M. Bubnov, and M. E. Likhachev, Proc SPIE. **10897**, 67 (2019).
22. K. Bobkov, A. Andrianov, M. Koptev, S. Muravyev, A. Levchenko, V. Velmiskin, S. Aleshkina, S. Semjonov, D. Lipatov, A. Guryanov, A. Kim, and M. Likhachev, Opt. Express **25**, 26958 (2017).
23. M. M. Khudyakov, A. S. Lobanov, D. S. Lipatov, A. N. Abramov, N. N. Vechkanov, A. N. Guryanov, M. A. Melkumov, K. K. Bobkov, S. S. Aleshkina, T. A. Kochergina, L. D. Iskhakova, F. O. Milovich, M. M. Bubnov, and M. E. Likhachev, Laser Phys. Lett. **16**, 025105 (2019).